Chapter 1

Experimental Structural Dynamics - Acquisition of FRFs

1.1 Experimental tests of dynamic analysis

The experimental tests of dynamic analysis, which can be carried out on single structural elements and also on an aircraft or on a complete space system, have as their main objective the evaluation of the response of the structure to stresses and the possibility of verifying and, if necessary, of developing a numerical model to precidt the dynamic behavior of the structure. In general, however, experimentation is conducted with input stresses that do not correspond to any typical working condition.
The term *modal analysis* refers to the experimental process of acquiring data that enables a numerical description of the dynamic behavior of a structure to be determined.
Although the fundamental purpose of a dynamic experimentation is always to obtain a numerical model of the structure, there are differences which relate to the intended use of the model itself. These differences are important from an experimental point of view because they determine the precision required for experimentation and thus the "difficulty" and ultimately the " cost". The model can be used for:

- *validation of the numerical model* of the structure: in this case it is necessary to obtain a very precise evaluation of the fundamental frequencies and a description of the modal deformations which is sufficient to identify the type of mode; as far as the damping coefficients are concerned, a comparison with the values obtained from a numerical prediction is generally not possible, but only with rough estimates obtained by analogy of known values for structures with similar characteristics;

- *search for the causes of the differences* between the numerical model and the experimental data: compared to the previous case, a more accurate evaluation of the modal deformations and the acquisition of a higher number of fundamental modes are required;

- *identification of a numerical model* to be used also for *substructuring techniques*, *structural modification*, for the identification of the forces acting on the structure or for the identification of damages occurring during the working life: in all these cases, a greater level of precision in the measurements and the determination of an even higher number of fundamental modes are required.

In the general case the dynamic model of a structure is given by a discrete system with multiple degrees of freedom, it represents an approximation of the actual situation which is that of a continuous structure and therefore characterized by an infinite number of degrees of freedom; in the case of viscous damping, the equation of the system with n degrees of freedom is:

$$\mathbf{M}\ddot{\mathbf{x}} + \mathbf{C}\dot{\mathbf{x}} + \mathbf{K}\mathbf{x} = \mathbf{f}(t) \tag{1.1}$$

where $\mathbf{x}$ is a vector, of n components, which includes the degrees of freedom chosen for the representation of the structure (from the experimental point of view they are the measurement points), $\mathbf{f}(t)$ is the vector of the forces acting on the structure, $\mathbf{M}$ is the mass matrix, $n \times n$, and analogously $\mathbf{C}$ and $\mathbf{K}$ are the viscous damping and stiffness matrices, $n \times n$.
As seen in Cap. **??**, three types of dynamic description can be defined:

- spatial, $\mathbf{K}$, $\mathbf{M}$, $\mathbf{C}$ matrices;
- modal, $\mathbf{\Phi}$, $\mathbf{\Omega}^2$, $\mathbf{\Lambda}^2$ matrices;
- of frequency response functions, $\mathbf{H}(\omega)$ matrix.

In the field of the experimental technique of dynamic analysis, reference will essentially be made to a methodology that concerns the determination of the frequency response functions, indicated with FRF, by means of the excitation of the structure at a single point and the detection of the output at another measurement point (it is also possible a different situation in which both the input and the output can be relative to more than one point of the structure); experimentation directly provides a response model in terms of the *frequency response functions*. From the evaluation of an appropriate number of $FRFs$ it is possible to pass to the modal or spatial model.
The input signalby connecting the structure with a " shaker " or more simply with an impulsive input, generally obtained with a hammer equipped with a load cell, while the transducer generally used for the output quantity is an accelerometer which must be connected to the structure: it constitutes therefore an "alteration" of the structure itself. This alteration must be minimised, therefore the mass of the accelerometer must be as small as possible; this requirement is, as said, compatible with the use of piezoelectric accelerometers.
Also in the application of excitation forces there is an alteration of the structure, in particular in the case of the use of "shakers".

1.2 Determination of FRFs with general input

Reference is now made to the more general case in which the input signal and therefore the response signal are not simple harmonics.

1.2.1 Periodic input

In this case the input signal is periodic with period T. Let us consider for simplicity a system with a single input and a single output (*SISO*, Single Input Single Output); the input signal can be expressed with a Fourier series development, in fact a periodic function with period T can

be developed as follows:[1]

$$f(t) \;=\; \sum_{k=-\infty}^{+\infty} f_k^* e^{j\omega_k t} \tag{1.4}$$

with $\omega_k \;=\; 2\pi k/T$.
The response signal $x(t)$ can be evaluated by considering the meaning of the FRF and therefore using the FRF calculated at the frequencies that are present in the input signal, $f(t)$, as shown in 1.4:

$$x(t) \;=\; \sum_{k=-\infty}^{+\infty} x_k^* e^{j\omega_k t} = \sum_{k=-\infty}^{+\infty} H(\omega_k) f_k^* e^{j\omega_k t} \tag{1.5}$$

Of course, the response signal contains only those frequencies which are included in the input signal: therefore the response signal $x(t)$ is periodic, with the same period T as the input signal, but has a different form because the FRF has different values depending on the frequency.
To determine the FRF in the case of a periodic input it is therefore necessary to calculate the Fourier series developments of the input and output signals: the components of the input and output functions for the same discrete frequency values that are integer multiples of $2\pi/T$ are thus obtained. From these components we derive the FRFs at the only discrete frequencies that are multiples of $2\pi/T$:

$$H(\omega_k) \;=\; \frac{x_k^*}{f_k^*} \tag{1.6}$$

From 1.6 the FRFs can be obtained at the frequency values corresponding to multiples of the input signal. This procedure can of course be extended for multiple input and multiple output systems (*MIMO*, Multiple Input Multiple Output), if there are several measurement points. In this case, the generic term of the FRF matrix is:

$$H_{ij}(\omega_k) \;=\; \frac{x_{k_i}^*}{f_{k_j}^*} \tag{1.7}$$

for which the periodic input must be applied at the $j-th$ point $j-imo$ and must zero at all other points.

[1] The 1.4 is the complex (exponential) form of the Fourier series: the coefficients f_k^* are given by the expression:

$$f_k^* \;=\; \frac{1}{T}\int_0^T f(t)\; e^{-j\omega_k t} dt \tag{1.2}$$

By expressing the complex exponential with trigonometric functions using Euler's formula, we get this expression for the monolateral Fourier series:

$$f(t) \;=\; \frac{a_0}{2} + \sum_{k=1}^{+\infty} \left[a_k \cos(\omega_k t) + b_k \sin(\omega_k t)\right] \tag{1.3}$$

1.2.2 Impulsive input

Let us consider again a system with single input and single output, $SISO$. In the case in which the input signal is of the generic type (at the impulsive limit), it can be considered that the Direchlet condition is respected:

$$\int_{-\infty}^{\infty} |f(t)|dt \ < \infty \tag{1.8}$$

and it is therefore possible to define and calculate the Fourier transform of this signal defined as (the Fourier-transformed quantities are indicated with the symbol ˜):

$$\tilde{f}(\omega) \ = \ \int_{-\infty}^{\infty} f(t)e^{-j\omega t}dt \tag{1.9}$$

at each pulse ω, we can write for the response signal:

$$\tilde{x}(\omega) \ = \ H(\omega) \ \tilde{f}(\omega) \tag{1.10}$$

where $H(\omega)$ indicates the FRF. The response signal $x(t)$ can therefore be obtained from the inverse Fourier transform of the relation 1.10:

$$x(t) \ = \ \frac{1}{2\pi}\int_{-\infty}^{\infty} H(\omega)\tilde{f}(\omega)e^{j\omega t}d\omega \tag{1.11}$$

FRFs can therefore be obtained from dynamic analysis tests with impulsive excitation: it is a matter of calculating the Fourier transforms of the input and output signals and obtaining the FRFs as a ratio of these two functions:

$$H(\omega) \ = \ \tilde{x}(\omega)/\tilde{f}(\omega) \tag{1.12}$$

For systems with several inputs and outputs, we will still have

$$H_{ij}(\omega) \ = \ \frac{\tilde{x}_i(\omega)}{\tilde{f}_j(\omega)} \tag{1.13}$$

in which the Fourier transformed vector of the input $\tilde{f}_i(\omega)$ $(i = 1, 2, ..., n)$ is non-zero only at the $j-th$ measurement point. From a numerical point of view, the Fourier transforms of the input and response signals are calculated by evaluating the discrete Fourier transforms, with a numerical process referred to as FFT, Fast Fourier Transform; this numerical procedure implies that the signal is treated as a periodic signal.
The case of impulsive excitation can be treated differently by evaluating the response of a system to a unitary impulse ($f(t) = \delta(t)$), Duhamel's method. If we indicate with $h(t-\tau)$ the impulse response function and consider a generic input function $f(t)$, it is possible to express it through a linear combination of impulses $f(\tau)d\tau$. The response of the system is given by:

$$x(t) \ = \ \int_{-\infty}^{\infty} h(t-\tau)f(\tau)d\tau \tag{1.14}$$

where $h(t-\tau) = 0$ for $t < \tau$. The Fourier transform of a unitary pulse $\delta(t)$ is:

$$\tilde{f}(\omega) \ = \ \int_{-\infty}^{\infty} f(t)e^{-j\omega t}dt = \int_{-\infty}^{\infty} \delta(t)e^{-j\omega t}dt = 1 \tag{1.15}$$

placing 1.15 in 1.11, we have:

$$x(t)_\delta \;=\; h(t) \;= \frac{1}{2\pi}\int_{-\infty}^{\infty} H(\omega)\tilde{f}(\omega)e^{j\omega t}d\omega \;=\; \frac{1}{2\pi}\int_{-\infty}^{\infty} H(\omega)e^{j\omega t}d\omega \tag{1.16}$$

as we can see from 1.16, the impulsive response $h(t)$ and the FRF of the system $H(\omega)$ are a pair of Fourier transforms; this means that the impulsive response of the system, $h(t)$, is obtained from the anti-Fourier transform of the FRF, i.e. of the $H(\omega)$.
From this correspondence between impulsive response and FRF, it can be seen that it is possible to express the impulse response function with a series development on a modal basis, as it happens for FRF; in fact from:

$$H_{ij}(\omega) \;=\; \sum_r H_{ij}^r(\omega) = \sum_r -\frac{\phi_i^{(r)}\phi_j^{(r)}}{-m_r\omega^2 + k_r + j\omega c_r} \tag{1.17}$$

we have correspondingly:

$$h_{ij}(t) \;=\; \sum_r h_{ij}^r(t) \tag{1.18}$$

1.2.3 Random input

In this case, which is very important for the possibilities it offers in experimentation, the input signal and therefore the output signal are random: the Dirichlet condition is not respected and therefore it is not possible to apply the definition of the Fourier transform for input and output signals.
A random signal is defined with a statistical approach since the single signal, unlike in the deterministic field, is not significant. The random character, in modal analysis, refers to the fact that a series of experiments, even if carried out in an apparently equal manner and under the same circumstances, leads to different results. Therefore the result of a single test is not sufficient to represent the measure, but a statistical description of the results is required.
Different methods must be used to describe the signals: this can be done in the time domain by means of the correlation function and in the frequency domain by means of the spectral density function, PSD (Power Spectral Density), see App. **??** for theoretical remarks on random processes.
A random signal is defined as stationary if its statistical properties, in particular the average, do not change over time. The avarage of an *ergodic* random signal, i.e. with time averages equal to the averages calculated on the set of samples and thus such that its properties can be assessed by a single recording of sufficiently large duration, is defined by:

$$\overline{x} = \lim_{T\to\infty}\frac{1}{T}\int_0^T x(t)dt \tag{1.19}$$

The mean square value of the random signal is defined by:

$$\overline{x}^2 = \lim_{T\to\infty}\frac{1}{T}\int_0^T x^2(t)dt \tag{1.20}$$

In the case of random signals this value is also referred to as variance and gives an indication of the magnitude of variation of the signal $x(t)$.

Arelated quantity is the square root of the variance, the square root of the mean square value x_{rms} (root mean square):

$$x_{rms} = \sqrt{\overline{x}^2} \tag{1.21}$$

Another important index in the field of random variables is the measure of the variation over time of the signal, which allows to evaluate the size of the statistical sample of the signal to be collected. The autocorrelation function, indicated with $R_{xx}(\tau)$, is defined by:

$$R_{xx}(\tau) = \lim_{T\to\infty} \frac{1}{T} \int_0^T x(t)x(t+\tau)dt \tag{1.22}$$

it gives an indication on the speed of variation of the signal $x(t)$ and is only a function of τ, the time difference, in the case of stationary random signals.
The correlation function between the signals $f(t)$ and $g(t)$ (or autocorrelation if referred to the same signal) has the physical meaning of mean value of the product of the function $f(t)$ for a function $g(t)$ shifted in time: $f(t) * \quad g(t+\tau)$; it is always a function of time that responds however to the conditions required to define its Fourier transform; for example in the case of autocorrelation for the signal $f(t)$ we have:

$$R_{ff}(\tau) \;=\; E\left[f(t)\; f(t+\tau)\right] \tag{1.23}$$

where the symbol $E\left[...\right]$ stands for the expected value of the quantity in brackets: under the hypothesis that the signal is *stationary* from a statistical point of view (i.e., that all the probability characteristics are independent of temporal translations) and is also *ergodic*, i.e., that the time averages are equal to the averages calculated on the set of samples, 1.23 can be expressed as:

$$R_{ff}(\tau) \;=\; E\left[f(t)\; f(t+\tau)\right] = \lim_{T\to\infty} \frac{1}{T} \int_0^T f(t)\; f(t+\tau)dt \tag{1.24}$$

and therefore each stochastic function $f(t)$ is completely representative of the random process.
The Fourier transform of the autocorrelation function, indicated by 1.23, defines a spectral self-density function:

$$S_{ff}(\omega) \;=\; \int_{-\infty}^{\infty} R_{ff}(\tau)e^{-j\omega\tau}d\tau \tag{1.25}$$

through this spectral density function, a description in the frequency domain of the time function $f(t)$ is obtained. The random signal characteristic of $f(t)$ does not allow classical definition of Fourier transform o be applied directly to the function itself.
The definitions given in 1.23, 1.25 extend naturally to the case of two functions $x(t)$, $f(t)$ for which a correlation or cross-correlation function is defined:

$$R_{xf}(\tau) \;=\; E\left[x(t)\; f(t+\tau)\right] = \lim_{T\to\infty} \frac{1}{T} \int_0^T x(t)\; f(t+r)dt \tag{1.26}$$

and consequently a spectral density or cross-density spectral function is defined:

$$S_{xf}(\omega) \;=\; \int_{-\infty}^{\infty} R_{xf}(\tau)e^{-j\omega\tau}d\tau \tag{1.27}$$

It is observed that the correlation functions defined by 1.23, 1.26 are real functions [2] and also the spectral self-density functions are real functions while the spectral cross-density functions are, in general, complex functions but such that it is:

$$S_{xf}(\omega) \;=\; S^*_{fx}(\omega) \tag{1.28}$$

where * indicates the complex conjugate.
In this way we have defined, through correlation operations and Fourier transforms on the correlation functions, the functions that allow us to deal with random signals. Then there is a relation that connects the spectral auto-density functions of the input and output signals with the FRF of the system:

$$S_{xx}(\omega) \;=\; |H(\omega)|^2 S_{ff}(\omega) \tag{1.29}$$

This relationship alone is not sufficient for the evaluation of the FRF of the system as it only provides information about the modulus of $H(\omega)$, therefore further relationships involving also the spectral cross-density functions must be used. As mentioned above, the spectral cross-density functions are complex and therefore allow us to derive the $H(\omega)$ in complex form:

$$S_{fx}(\omega) \;=\; H(\omega) S_{ff}(\omega) \tag{1.30}$$

$$S_{xx}(\omega) \;=\; H(\omega) S_{xf}(\omega) \tag{1.31}$$

Relations 1.30, 1.31 allow to derive the FRF of the system starting from experimental measurements carried out with a random input signal; from these two relations we obtain two possible estimates for the function $H(\omega)$ and from the comparison of these two different estimates the quality of the obtained experimental data can also be evaluated (see beyond Sec. 1.3.4).

1.3 Use of different inputs

Experimental modal analysis tests can be performed with different types of input signals; they have some advantages and some drawbacks that are presented in the following subparagraphs.

1.3.1 Sinusoidal input with discrete frequency variation

In this case the input signal is simple harmonic with fixed amplitude and frequency and the FRF is measured point by point for each frequency value considered, see par. 1.2.1.
So, to obtain a single FRF of the system, the frequency of the input signal has to be varied in a discrete way. Of course, the measurement requires that steady-state conditions are reached when passing from one frequency to another, and this can take a long time to measure. In practice, the time required becomes critical around a resonance frequency when the modal damping coefficient is very low.
An advantage offered by the use of this type of input lies in the possibility of " spacing " the frequency in the measurement in the way considered most appropriate: thus it is possible to collect few frequency measurement points for frequencies that are far from the resonance points

[2] Note that for example, the R_{ff} defined with the 1.24 is an even function, so doing the transform 1.25 with $e^{-j\omega t} = \cos(\omega t) - j\sin(\omega t)$e have as unique by integrating not $R_{ff}\cos(\omega t)$ that give rise to a S_{ff} real.

of the system and to concentrate the maximum number of the frequency measurement around the resonance points, thus obtaining the most significant data for the subsequent evaluation of modal parameters.
Measuring with this type of input involves a two-step process:

- a first exploration is conducted with a large frequency range and aims to identify resonance points;
- the second phase is carried out around the resonance peaks with very small frequency increments in order to collect the most significant data relating to the individual modes.

1.3.2 Sinusoidal input with continuous frequency variation

It is a case similar to the previous one, the input signal is still pure harmonic, but the frequency variation of the signal is continuous (see parr. 1.2.1 and 1.2.2); of course, it must always be verified that this frequency variation is sufficiently to maintai stationary conditions in the measurement.
In fact, a too high frequency change rate leads to very significant distortions in the FRF evaluation, the admissible rate of variation is conditioned by the modal damping coefficient values; special standards set the maximum values of the rate of frequency variation.
With this type of input a continuous frequency "brushing" is obtained from a fixed initial and final frequency value.

1.3.3 Periodic input

In the case of a periodic input signal, we have a discrete set of frequencies contained in the signal itself. From the evaluation of the Fourier transforms of the input and output signals, which are periodic (v. par. 1.2.1), we get the FRFs of the system from the relations 1.6 and 1.7. In order to obtain periodic input signals it is possible to use deterministic signals, such as square waves, or pseudo-random signals. An important advantage offered by this type of input, compared to the previous case of a simple harmonic input, is given by its periodicity that allows to obtain from a single measurement the information relative to a frequency range, chosen by the operator, with a fixed frequency increase.

1.3.4 Random input

In the case of random input, we have, as we have seen, three different relationships that allow us to evaluate the FRF of the system:

$$S_{xx}(\omega) = |H(\omega)|^2 S_{ff}(\omega) \tag{1.32}$$

$$S_{fx}(\omega) = H(\omega) S_{ff}(\omega) \tag{1.33}$$

$$S_{xx}(\omega) = H(\omega) S_{xf}(\omega) \tag{1.34}$$

where $H(\omega)$ denotes the FRF of the system and the functions $S(\omega)$ denote the spectral density functions, PSD.

The basic measurement tool in modal analysis is typically a two-channel analyzer. It is able to calculate in an approximate form with different numerical procedures the different functions that appear in 1.32, 1.33, 1.34. In all cases, spectral density functions cannot be evaluated exactly if one has, as is obviously inevitable in measurement, a data set of finite time duration.
In the case of a random input signal, FRFs can be evaluated with different estimates; if we indicate with $H^1(\omega)$ the FRF obtained from 1.33, we have:

$$H^1(\omega) \;=\; S_{fx}(\omega)/S_{ff}(\omega) \tag{1.35}$$

if we indicate with $H^2(\omega)$ the FRF obtained from the 1.34, we have:

$$H^2(\omega) \;=\; S_{xx}(\omega)/S_{xf}(\omega) \tag{1.36}$$

of course the functions $H^1(\omega)$, $H^2(\omega)$ that are calculated from different experimental data will have different values and not exactly equal to the ones they should theoretically assume. Thus, to assess the reliability of the measurement process, a *coherence function*, indicated with γ, is defined by:

$$\gamma^2 \;=\; H^1(\omega)/H^2(\omega) = \frac{S_{fx}(\omega)S_{xf}(\omega)}{S_{ff}(\omega)S_{xx}(\omega)} \tag{1.37}$$

It can be verified that this function γ must always have a value less than or equal to one and that $\gamma = 1$ corresponds to the ideal conditions of measurement in which the frequency response functions $H^1(\omega)$ and $H^2(\omega)$ are equal.
Of course, the presence of noise in the input and output signals disturbs the measurement: in the neighborhood of a resonance frequency the effect of the noise is very important on the input signal and therefore it alters the spectral density function relative to the input, $S_{ff}(\omega)$, while in the neighborhood of an anti-resonance points, where the response signal is reduced to a minimum, the noise has a greater effect on the response signal and therefore it alters mainly the spectral density function of the output signal $S_{xx}(\omega)$.
Hence, around resonance points the $H^2(\omega)$ function is likely to give the most reliable estimate for the measurement, while on the contrary around anti-resonance points the $H^1(\omega)$ function is likely to give the best estimate.
It is observed that very low values of the coherence function γ, which make the measurement unacceptable, can be caused by a non-linear behavior of the structure and therefore can be considered as a possible index of non-linear behavior; another cause for too low values of the coherence function is connected with an insufficient frequency resolution, which depends on the digitization process and therefore on the frequency measurement points that are available, especially in the modal analysis of structures characterized by very small damping coefficient values. This second observation suggests a repetition of the measurement with the use of a higher number of frequency sampling points.

1.3.5 Impulsive input

In this case the input signal can be obtained in a different way with:

- a rapid change in frequency of a sinusoidal signal, which is indicated with the term *chirp*;
- a rectangular pulse over time.

The first is the case of a harmonic excitation with a frequency varying from a minimum value, f_{min}, to a maximum value, f_{max}. In this way, it is possible to obtain a very precise control over both the limits of the frequencies contained in the impulsive signal and the amplitudes of the signal, and it is also possible to obtain a high energy and therefore a very high signal-to-noise ratio.
In the second case the impulsive signal is obtained with an excitation of limited duration, for example with the use of a "hammer" with a load cell that allows to measure the force transmitted to the structure: the control of the frequency band of the signal and of its amplitude is much less direct and precise than in the case of the chirp, moreover the available energy is limited, but there is the advantage of using a very simple instrumentation.
From this impulsive excitation we can calculate the Fourier transforms for the input and the output , with the numerical use of the FFT, and then we can derive the FRFs from 1.12 and 1.13. In the case of random input, it is also possible to use the previously defined relations 1.30, 1.31 and then go through the calculation of the correlation functions and of the spectral density functions.
Modal analysis tests based on the use of the impulsive type of input have some advantages both with regard to the simplicity and versatility of the instrumentation and with regard to the measurement technique, but also have several drawbacks in particular with regard to the precision of the measured data, generally lower than that obtainable with other types of input, of the measured data and the difficulty of use on large structures.

1.3.6 The excitation system

The excitation system can have different structures, but basically it is a *shaker* (electromagnetic or electro-hydraulic type) or a *hammer with a load cell*.

- In the case of *electromagnetic shaker*, the excitation signal can be random, sinusoidal with continuous frequency variation and many other types. The electromagnetic shaker consists of a coil placed around a shaft in a magnetic field: by applying an alternating current, a force is applied to the shaker shaft, which in turn transfers the force to the structure.
  Of course, this excitation system must be connected to the structure under test and there is therefore an insertion effect which can be relevant according to the masses involved.
  This effect is reduced by connecting the shaker to the structure via a *stinger*, which is a short, thin rod (often made of steel or nylon): this rod isolates the shaker from the structure, reduces the effect of added mass effect and allows to control the direction of force application.

- The use of *the hammer with load cell* avoids the issues of added mass and allows a much faster experimentation. It is a hammer with a force transducer on the impact section: it is used to give the structure a broadband impulse excitation which is the larger the longer the time duration of the impulse.[3] In Fig. 1.1 the trend as a function of time and the trend as a function of frequency of a typical impulse are shown. The peak value of the

[3]This statement can be easily proved by considering a "quasi-pulse" δ_b consisting of a rectangular pulse centered in the origin of times with "base " b and height $1/b$ so that it has integral equal to one. Its Fourier transform is equal to:

$$\mathcal{F}[\delta_b] = \int_{-b/2}^{b/2} \frac{1}{b} e^{-j\omega t} dt = \frac{1}{-jb\omega} \left[e^{-j\omega b/2} - e^{j\omega b/2} \right] = \frac{2}{b\omega} \sin\left(\omega \frac{b}{2}\right) \tag{1.38}$$

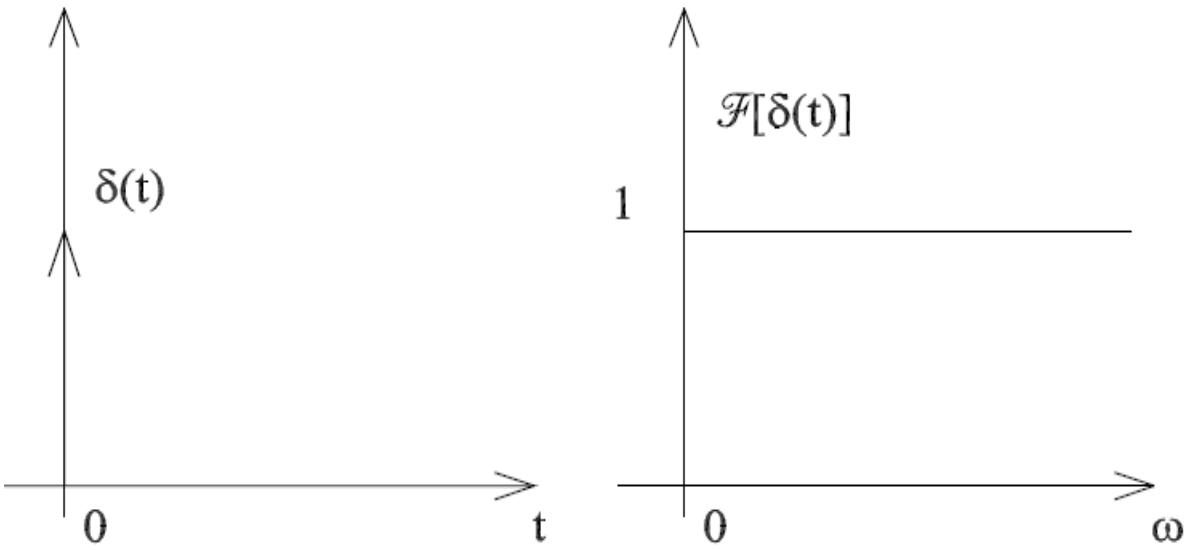

Figure 1.1: Impulsive input over time and its Fourier transform.

force depends on the mass of the hammer and the impact velocity: the load cell placed on the impact head allows the impact force to be measured.
The duration of the impulse, its frequency content and therefore the maximum excitation frequency, depend on the mass and stiffness of the hammer and of the structure under test.
The maximum excitation frequency decreases as the mass of the hammer increases and increases as the stiffness of the hammer tip increases.
Although the simplicity of using the hammer is obvious, it may be impossible to give a structure, in particular a large one, sufficient energy for excitation and also the direction of application of the force may be uncertain.

1.4 Determination of modal parameters from FRFs: SDOF hypothesis

The determination of the modal parameters, which are *the natural frequencies, the modal damping coefficients and the modal deformations*, from experimental data, which are the FRFs, requires a preliminary choice between a simple approach, based on the idea that it is possible to isolate the single mode in the neighborhood of the resonance frequency and then consider a modal reconstruction based on the single degree of freedom model (SDOF), and a more general approach, which is certainly necessary in the case of coupled modes, based on a modal reconstruction with a multi degree of freedom model (MDOF). In other words, if we consider the expression of a generic term of the FRF matrix as a function of the modal parameters and

The previous one shows that the non-ideal impulse over time has a spectrum which is a function like $\sin x/x$ which is basically constant in the origin and which tends to diminish until it vanishes at $\omega = 2\pi/b$ which therefore defines the bandwidth.

under the hypothesis of viscous damping

$$H_{ij}(\omega) = \sum_{r=1}^{N_{modi}} \frac{\phi_i^{*(r)} \phi_i^{*(r)}}{-\omega^2 + \omega_r^2 + j2\omega\omega_r\zeta_r} \tag{1.39}$$

it can be considered, in a neighborhood of ω close to the $p-ma$ resonance, that only the fraction $p-ma$ of Eq. 1.39 partecipates (hypothesis SDOF) or we must consider the influence of all the other contributions.
The hypothesis of being able to work on a model with only one degree of freedom requires that the modes are well separated in frequency and not strongly damped, because in this case a coupling is created even between modes that are relatively far apart in frequency. However, even the presence of very low modal damping coefficients leads to problems for the determination of the modal parameters, because in this case there are few significant points in the neighborhood of the resonance frequency, while for a good reconstruction of the modal parameters it would be useful to have a large number of relevant measurements points (at least a dozen) around each resonance frequency.
The approach based on the single degree of freedom model is however useful at least to obtain a first estimate of the modal parameters that can then be evaluated with greater precision by more sophisticated methods. In this case the fundamental steps are:

- *The natural vibration frequency* is identified. The point correspondi to the local maximum of the modulus of the FRF as a function of the frequency is considered as the natural frequency of the mode, f_n; it is observed that this value is found in every element of the FRF. It can also be identified looking for the crossing points of the frequency axis of the real part of the FRF or through the points where the imaginary part has relative minima or maxima.

- As far as the estimation of *modal damping* is concerned, let us take into account the following considerations: if, as assumed by hypothesis, we consider the single degree of modal freedom, the average power P_m dissipated by the viscous force in a simple harmonic motion cycle induced by a forcing $f(t) = F_0 \sin(\omega t)$ would be: [4]

$$P_m(\omega) := \frac{1}{T}\int_0^T c\dot{x}^2 dt \;=\; \frac{1}{2} c_c \omega^2 \frac{F_0^2}{k^2} \frac{\zeta_n}{\left[1 - \left(\frac{\omega}{\omega_n}\right)^2\right]^2 + 4\zeta_n^2 \left(\frac{\omega}{\omega_n}\right)^2} \tag{1.42}$$

  in which each dynamic quantity has modal meaning and $c := \zeta_n c_c$. This average power is *maximum* when $\omega = \omega_n$, as it can be easily verified looking for the ω that satisfies

[4] In that case, by the very meaning of FRF it would be

$$x(t) = F_0 \left|H(\omega)\right| \sin(\omega t + \psi) \qquad \dot{x}(t) = F_0 \omega \left|H(\omega)\right| \cos(\omega t + \psi) \tag{1.40}$$

with $H(\omega) = 1/k \left[1 - (\omega/\omega_n)^2 + j2\,(\omega/\omega_n)\,\zeta_n\right]$ and so,

$$\left|H(\omega)\right|^2 = \frac{1}{k^2 \left\{\left[1 - \left(\frac{\omega}{\omega_n}\right)^2\right]^2 + 4\zeta_n^2 \left(\frac{\omega}{\omega_n}\right)^2\right\}} \tag{1.41}$$

$dP_m(\omega)/d\omega = 0$.

$$P_{m_{max}} := \frac{1}{8} c_c \omega_n^2 \frac{F_0^2}{\zeta_n k^2} \tag{1.43}$$

If we look for the values of ω for which P_m is the " half " of its maximum value (from which the term of *half-power points*), we would impose that $P_m(\omega)$, given by Eq. 1.42, is equal to $P_{m_{max}}/2$ (see Eq. 1.43). Thus proceeding, we get:

$$\left[1 - \left(\frac{\omega}{\omega_n}\right)^2\right]^2 - 4\zeta_n^2 \left(\frac{\omega}{\omega_n}\right)^2 = 0 \quad \rightarrow \quad \left(\frac{\omega}{\omega_n}\right)^2 \pm 2\zeta_n \left(\frac{\omega}{\omega_n}\right) - 1 = 0 \tag{1.44}$$

whose four roots, depending on the two different choices for the sign, are:

$$\left(\frac{\omega}{\omega_n}\right)_{1,2} = -\zeta_n \pm \sqrt{\zeta_n^2 + 1} \qquad \left(\frac{\omega}{\omega_n}\right)_{3,4} = +\zeta_n \pm \sqrt{\zeta_n^2 + 1} \tag{1.45}$$

Owing to the nature of its coefficients (a variation and a permanence of sign), however, each second-degree equation must have a positive and a negative root. Then, the smallest (real) root is eliminated for each set of solutions:

$$\left(\frac{\omega}{\omega_n}\right)_{2,4} = \mp\zeta_n + \sqrt{\zeta_n^2 + 1} \tag{1.46}$$

If we rename then these two roots with ω_1 and ω_2, we get ζ_n easily by difference[5]

$$\zeta_n \;=\; \frac{\omega_2 - \omega_1}{2\omega_n} \tag{1.48}$$

which represents an estimate of the viscous damping based on the frequencies ω_1 and ω_2: it remains now to say how to evaluate ω_1 and ω_2 based on the knowledge of $H(\omega)$. In the following two possible ways are presented: one based on the knowledge of the modulus of $H(\omega)$ and the other on the knowledge of its real part.

– Indicating with $|H|^2_{mp}$ the value assumed by the modulus of the FRF at the two roots, we have, considering Eq. 1.41 and the first of Eq. 1.44:

$$|H|^2_{mp} = \left.\frac{1}{k^2 \left\{\left[1 - \left(\frac{\omega}{\omega_n}\right)^2\right]^2 + 4\zeta_n^2 \left(\frac{\omega}{\omega_n}\right)^2\right\}}\right|_{\omega=\omega_1,\omega_2} = \left.\frac{1}{k^2 8\zeta_n^2 \left(\frac{\omega}{\omega_n}\right)^2}\right|_{\omega=\omega_1,\omega_2} \tag{1.49}$$

Finally, observing from Eq. 1.41 that $|H|^2_{max} = |H(\omega)|^2_{\omega=\omega_n} = 1/4k^2\zeta_n^2$ and considering Eq. 1.46, we get:

$$|H|^2_{mp} = \frac{1}{k^2 8\zeta_n^2 \left(1 + 2\zeta_n^2 \mp 2\zeta_n\sqrt{\zeta_n^2 + 1}\right)} \simeq \frac{H^2_{max}}{2} \tag{1.50}$$

[5]Observe that we also have

$$\omega_n^2 \;=\; \omega_1\omega_2 \tag{1.47}$$

in which damping terms of order higher than the second have been neglected in the denominator. Therefore, starting from the maximum value of the modulus of FRF as a function of frequency, H_{max}, we evaluate the half-power points, of frequency f_1 and f_2, corresponding to the values $H_{max}/\sqrt{2}$ to the left and right of the peak value; Once the half-power points are known, the modal damping coefficient can be evaluated using Eq. 1.48 with the relations:[6]

$$\zeta_n = \frac{\eta_n}{2} \simeq \frac{D_f}{2f_n} \tag{1.52}$$

where D_f is *half power bandwidth*:

$$D_f \;=\; f_2 - f_1 \tag{1.53}$$

and where η_n is the loss factor related to the damping coefficient according to $\eta_n = 2\zeta_n$.

– The half-power points can also be determined by estimating the relative maximum and minimum points of the real part of $H(\omega)$ (see Fig. **??**). Indeed the real part (see Eq. **??**) is given by:

$$Re[H(\omega)] = \frac{(\omega_n^2 - \omega^2)}{m[(\omega_n^2 - \omega^2)^2 + 4\zeta_n^2\omega_n^2\omega^2]} \tag{1.54}$$

Therefore imposing:

$$0 \;=\; \frac{dRe[H(\omega)]}{d\omega} \tag{1.55}$$

the following equation is obtained:

$$0 \;=\; \left(\omega_n^2 - \omega^2\right)^2 \;-\; 4\zeta_n^2\omega_n^2 \tag{1.56}$$

which is identical to Eq. 1.44 (which shows that the roots found are actually half power points) and that has solutions ω_1 and ω_2:

$$\omega_1^2 \;=\; \omega_n^2\,(1 - 2\zeta_n) \qquad \text{per } \omega^2 < \omega_n^2 \tag{1.57}$$

$$\omega_2^2 \;=\; \omega_n^2\,(1 + 2\zeta_n) \qquad \text{per } \omega^2 > \omega_n^2 \tag{1.58}$$

Subtracting one from the other gives (see also Eq. 1.51 note):

$$\zeta_n = \frac{(\omega_2 + \omega_1)(\omega_2 - \omega_1)}{4\omega_n^2)} \tag{1.59}$$

which, considering the approximation $\omega_n = (\omega_1 + \omega_2)/2$, still provides the estimate given by Eq. 1.48.

[6] f the approximations made in neglecting higher order contributions were not taken into account, we would have obtained:

$$\zeta_n \;=\; \frac{[(f_2 + f_1)(f_2 - f_1)]}{4f_n^2} \tag{1.51}$$

Finally, it should be added that if instead of $H(\omega)$ (*receptance*) we had the response function in terms of acceleration $H_a(\omega)$ (*inertance*), as it is in usual in the measurements based on the use of accelerometers, we would have, for example in the case of the approach which uses the real part:

$$Re[H_a(\omega)] = \frac{-\omega^2(\omega_n^2 - \omega^2)}{m[(\omega_n^2 - \omega^2)^2 + 4\zeta_n^2\omega_n^2\omega^2]} \tag{1.60}$$

whose stationary points would be:

$$\omega_1^2 = \frac{\omega_n^2}{1+2\zeta_n} = \omega_n^2[1 - 2\zeta_n + \mathcal{O}(\zeta_n^2)] \tag{1.61}$$

$$\omega_2^2 = \frac{\omega_n^2}{1-2\zeta_n} = \omega_n^2[1 + 2\zeta_n + \mathcal{O}(\zeta_n^2)] \tag{1.62}$$

which shows that, apart from the usual approximations on the damping order, on the basis of the stationarity points of the real part of the receptance we obtain the same roots given by Eqq. 1.57 and 1.58.

- With regard to the estimation of *$r-th$ the modal shape at the N_{modes} experimental measurement points*, under the SDOF assumptions, let us consider that *a line of FRF* is known from the measurements, e.g. the first

$$H_{11}(\omega) \;\; H_{12}(\omega) \;\; H_{13}(\omega) \;\; ... \;\; H_{1N_{modi}}(\omega) \tag{1.63}$$

From Eq. 1.39, assuming ω_{n_r} and ζ_r to be known for the $r-th$ mode, we have for $\omega = \omega_{n_r}$:

$$H_{11}(\omega_{n_r}) \simeq \frac{\phi_1^{*(r)}\phi_1^{*(r)}}{j2\omega_{n_r}^2\zeta_r} \quad \rightarrow \quad \phi_1^{*(r)} = -\frac{2\zeta_r\omega_{n_r}^2}{\phi_1^{*(r)}}\; H_{I_{11}}(\omega_{n_r}) \tag{1.64}$$

in which we took into account the fact that at the resonance the real part of the FRF is zero. Applying analogous reasoning to the elements of the same row of the FRF matrix, it can be written:

$$H_{12}(\omega_{n_r}) \simeq \frac{\phi_1^{*(r)}\phi_2^{*(r)}}{j2\omega_{n_r}^2\zeta_r} \quad \rightarrow \quad \phi_2^{*(r)} = -\frac{2\zeta_r\omega_{n_r}^2}{\phi_1^{*(r)}}\; H_{I_{12}}(\omega_{n_r})$$

$$..... \tag{1.65}$$

$$H_{1N_{modi}}(\omega_{n_r}) \simeq \frac{\phi_1^{*(r)}\phi_{N_{modi}}^{*(r)}}{j2\omega_{n_r}^2\zeta_r} \quad \rightarrow \quad \phi_{N_{modi}}^{*(r)} = -\frac{2\zeta_r\omega_{n_r}^2}{\phi_1^{*(r)}}\; H_{I_{1N_{modi}}}(\omega_{n_r}) \tag{1.66}$$

Therefore by placing $c_r := -2\zeta_r\omega_{n_r}^2/\phi_1^{*(r)}$, we obtain for the components of the $r-th$ mode:

$$\left\{ \begin{array}{c} \phi_1^{*(r)} \\ \phi_2^{*(r)} \\ ... \\ \phi_{N_{modi}}^{*(r)} \end{array} \right\} = c_r \left\{ \begin{array}{c} H_{I_{11}}(\omega_{n_r}) \\ H_{I_{12}}(\omega_{n_r}) \\ ... \\ H_{I_{1N_{modi}}}(\omega_{n_r}) \end{array} \right\} \tag{1.67}$$

which shows that, apart from an essential c_r factor to its definition, the imaginary of a row of the FRF array evaluated at the resonance frequency provide an estimate of the

modal shape of the mode corresponding to the resonance itself.
It is also added that the same conclusions can be deduced if $FRFs$ with accelerations at the output are considered,[7] i.e., if, instead of Eq. 1.39, the following equation is considered:

$$H_{ij}(\omega) = \sum_{r=1}^{N_{modi}} \frac{-\omega^2 \ \phi_i^{*(r)} \phi_i^{*(r)}}{-\omega^2 + \omega_r^2 + j2\omega\omega_r\zeta_r} \tag{1.68}$$

In fact, retracing what was shown above, one would lead to a similar result given by Eq. 1.67 with the only difference that $c_r := 2\zeta_r/\phi_1^{*(r)}$ would be defined as constant.

Observations

Of course this approach has many limitations: it is evident from 1.51 that the estimation of the residual and of the modal damping factor depends on the evaluation of the peak value of the modulus of the FRF measured: in particular there are difficulties in the case of low damped modes beacuse of the very limited number of points available within the half power bandwidth. Even the basic assumption that the modes present in the frequency band chosen for the signal are considered as separate is not correct, because there is always a certain influence on the resonance behavior of the generic mode of all the fundamental modes, perceptible at least for the closest modes.
Several techniques have been proposed for the reconstruction of modal parameters. They are generally available on all the specialized software in the field of modal analysis, and allow, when necessary, to use a multi-mode model for the reconstruction of modal parameters.
It is observed that better evaluations of the modal parameters can be obtained by examining separately the real and imaginary part of the FRF in the neighborhood of the resonance. On one hand, the frequencies corresponding to the maximum points of the real part allow to evaluate the half power bandwidth and the resonance frequency more easily even if the problems related to the frequency resolution and the limited number of points available in the half power bandwidth remain. On the other hand, from the peak value of the imaginary part as a function of frequency a better estimate of the amplitude of the modal shape can be obtained.
As always, the evaluation of the resonance frequencies of the various modes present in the measured frequency band is simpler and more precise, while major problems are related to the determination of the modal shapes, which require a large number of measurement points and present greater uncertainties, and of the modal damping coefficients that, in general, tend to be overestimated. An inaccuracy of a fefw per thousand can be assessed for the measurement of resonance frequencies while much larger inaccuracies occurs for the evaluation of the damping coefficients.

1.5 Analyzer functions and signal analysis problems

The basic tool in the modal analysis field is the two-channel spectrum analyzer in the simplest configuration, which refers to a SISO (Single Input Single Output) system but which can be multi-channel for both input and output signals when referring to a MIMO (Multi Input Multi Output) system. This instrument is able to calculate different characteristics of the input and

[7] It should be noted that this eventuality is that which normally occurs in the practice of dynamic measurements due to the widespread use of accelerometric sensors.

output signals starting from the calculation of the discrete Fourier transform, FFT, from which it is possible to calculate the Fourier transforms and the spectral density functions which, as mentioned, are generally used for the evaluation of FRFs.
The input signal is discretized with an analogue digital converter, A/D, and then recorded as a succession of N values spaced by a sampling time, T_s, for a total observation time, indicated with T where $T = NT_s$.
If we accept the hypothesis, inherent in the use of the discrete Fourier transform, that the signal observed in time T is periodic with period T, we can calculate its discrete Fourier transform and thus obtain an estimate of the Fourier transform itself.
There are relations linking the signal observation time, T, the sampling pulsation, ω_s, the number of data points in time considered in the measure, N, the pulsation range considered for the signal spectrum, determined by ω_{max}, the pulsation resolution used in the signal analysis, $\Delta\omega$; in particular we have:

$$\omega_{max} \;=\; \omega_s/2 \;=\; 2\pi f_s/2 \;=\; 2\pi N/2T \;=\; \pi N/T \tag{1.69}$$

$$\Delta f = \frac{\Delta\omega}{2\pi} = \frac{\pi 2.56}{2\pi T} = \frac{1.28}{T} \tag{1.70}$$

in which the sampling theorem $\omega_s = 2\omega_{max}$ was used to avoid the aliasing phenomenon (see Par. 1.5.1). The frequency resolution (or step) is $\Delta\omega = \omega_{max}/N_R^*$, where N_R^* is the number of spectral lines, i.e. the frequency samples of the transformed provided by the FFT algorithm which are normally $N_R^* = N/2.56$.
The number of data in the time to be acquired in the measure, indicated with N, is fixed, generally with the possibility of different choices depending on the characteristics of the analyzer: this number almost always refers to powers of two and typical values are 1024, 2048, 4096, 8192, 16384, 32768 and therefore the frequency field, ω_{max}, and the resolution in pulsation, $\Delta\omega$, and in frequency, Δf, are related to the duration of the measure. The possibilities offered by industrial processors, e.g. 80486, now make it possible to work with very high N and thus obtain very small frequency resolutions.
It is observed from 1.70 that in order to obtain very small values for the frequency resolution it is necessary to work with very long observation times; if you have a very high number of measurement points, N, you have the advantage of acquiring measurements over a very wide frequency range, but the observation time required to obtain the fixed frequency resolution is only conditioned by 1.70 and therefore by the observation time T.
The necessity to use a long observation time, to obtain a good frequency resolution, can become a critical point in the experimentation, especially in the case of large space structures which are characterized by very low natural frequencies. In this case, in fact, the frequency resolution required for the measurement becomes very small and therefore the observation time becomes practically impossible; the problem is made even more difficult if the values of the modal damping coefficients are very low, due to the problem of truncation of the signal which is still relevant within the observation time.
Several aspects of digital analysis give rise to problems that are related to the approximations inherent in the discretization process and to the practical need to observe the signal for a finite and very limited acquisition time.
The relative problems are linked to the general problems of signal processing that go far beyond the specific field of modal analysis; these problems are of great practical importance and their knowledge may be necessary to acquire and use experimental data that are reliable. Some of

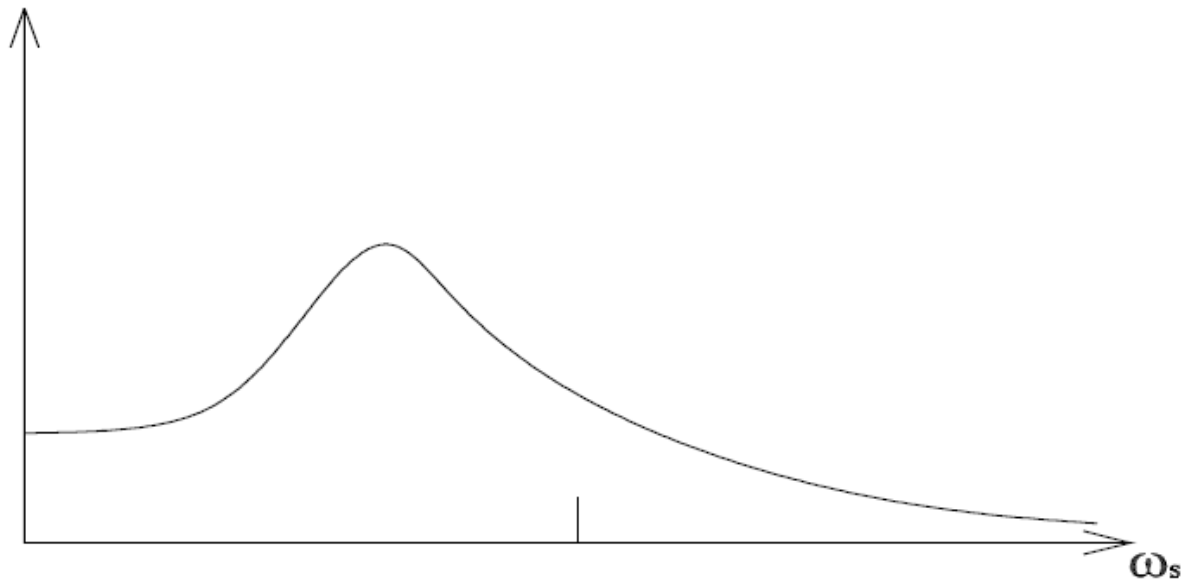

Figure 1.2: Module of the theoretical spectrum of a signal and its sampling frequency fixed ω_s.

these issues are outlined below in a very simplified form.

1.5.1 Aliasing

It is a phenomenon that is linked to the process of discretization of the continuous signal $x(t)$: if the frequency used for sampling the signal ω_s is:

$$\omega_s = 2\omega_{max} \tag{1.71}$$

if it is too low compared to the actual frequency composition of the signal[8] there is a distortion effect which is due to the significant presence of signal frequencies that are outside the bandwidht resultanting from the choice of the sampling frequency; this leads to the introduction of " false " low-frequency components that actually derive from out-of-band high-frequency components that are " reflected " inside the bandwidth, as shown in Figs. 1.2 and 1.3. In fact the sampling frequency, chosen according to the desired bandwidth, is not able to correctly reconstruct signals with $\omega > \omega_{max}$ which are mistakenly interpreted as signals with frequency $\omega^* < \omega_{max}$. The distortion in the signal spectrum can be explained by the fact that the components of the signal that have been "cut", i.e. which are at frequencies higher than half the sampling frequency, are reflected, hence the name "aliasing ", in the bandwidth chosen for the signal, between 0 and $\omega_s/2$.
In Fig. 1.2 the " real " spectrum of the signal is shown and in Fig. 1.3 the distorted spectrum, obtained from the sum of " true " and ' 'reflected " components is shown.
The solution to this problem is the use of " low pass " filters that " cut " and thus eliminate the frequencies present in the signal above the frequency range given by the choice of the

[8]Of course, in the case of continuous structures with an unlimited number of fundamental frequencies, modes with $\omega > \omega_{max}$ are always present.

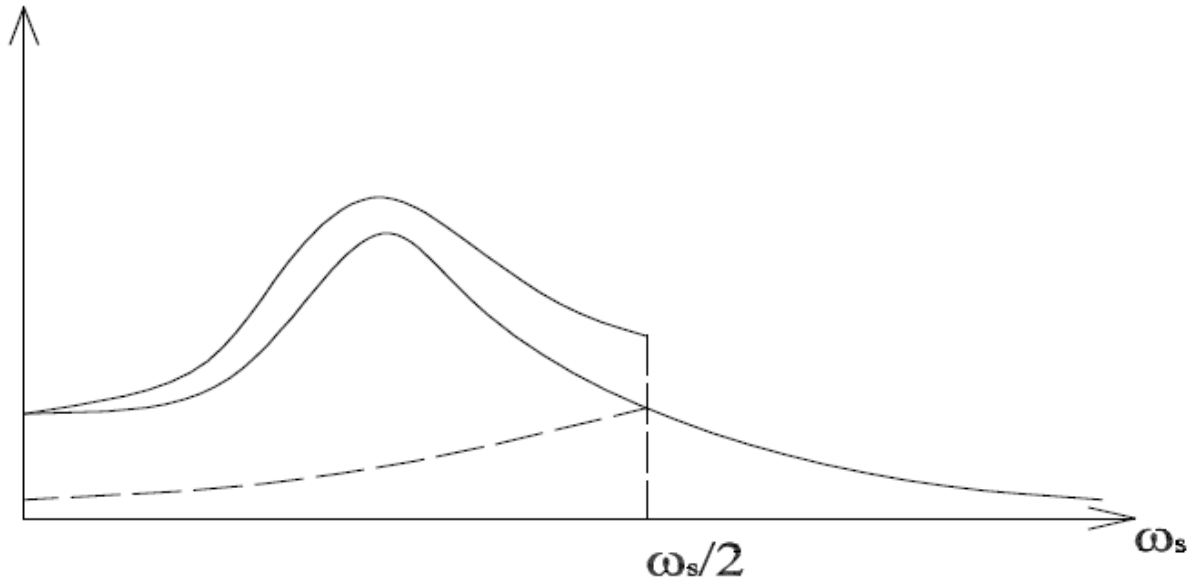

Figure 1.3: module of the theoretical spectrum of a signal and that of the actual spectrum evaluated by sampling the signal with frequency ω_s.

bandwidth. Generally the use of "anti aliasing" filters is automatically arranged with the choice of the analyser bandwidth, since the presence of these filters is absolutely necessary to obtain experimental data which are really usable in modal analysis: this problem is therefore generally "transparent" for the operator who does not have to perform any operation to eliminate this effect.

1.5.2 Leakage and windowing

This phenomenon is related to the limited duration of the observation time of the signal and to the fact that the signal, for the numerical evaluation of the FRF with the calculation of the FFT is considered as periodic with a period equal to the observation time T. If a simple harmonic signal is considered and if the duration of the observation time is such that it corresponds exactly with the period of the signal or with an integer multiple of periods, the effective spectrum is obtained, which in the example shown in Fig. 1.4 consists of a single line at the frequency, f_1, of the simple harmonic signal. If, on the contrary, the observation time does not exactly correspond to the period of the signal, as is generally the case, there is a discontinuity in the signal which is made periodic, but has no null value at the end of the period and there is a distortion in the spectrum. It has several lines, instead of just the frequency line at f_1 representing the "true" spectrum, and a "diffusion" of energy to other lines in the spectrum that is caused by the "discontinuity" in time due to the numerical process of periodicization. This procedure modifies the signal of interest by using another time signal before performing the Fourier transform so as to reduce the problem of "leakage": it essentially consists of zeroing the signal at the beginning and at the end of the observation time so as to eliminate the discontinuity created by periodisation.
If we denote by $w(t)$ the function of time that constitutes the window, then the signal that is

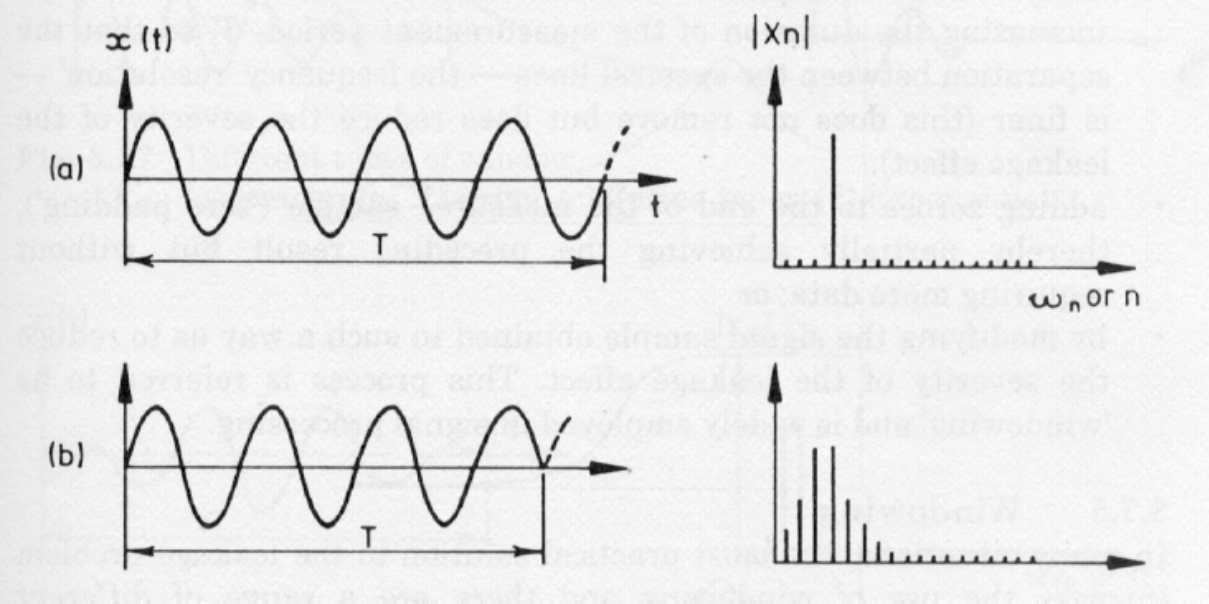

Figure 1.4: Signals with relative discrete spectra: dispersion effect (from Rif. [**?**]).

analyzed is given by the product of the signal under study, $x(t)$, and the time window $w(t)$:

$$x_w(t) \;=\; x(t)\; w(t) \tag{1.72}$$

that is, in the frequency domain:

$$\tilde{x}_w(\omega) \;= \int_{-\infty}^{\infty} \tilde{w}(\sigma)\tilde{x}(\omega-\sigma)d\sigma \tag{1.73}$$

In an analyzer there are always different functions are available for the time " windows", which can be of rectangular, exponential, Hanning's: they are chosen according to the type of the input signal: in some measurement systems it is also possible define, at the operator's choice, functions of time to be used as "windows" for particular purposes. In Fig. **??** some classic functions are shown. The four most commonly used windows are defined from the function:

$$\begin{aligned} w(t) \;&=\; a_0 - a_1\cos(\omega_0 t) + a_2\cos(2\omega_0 t) - a_3\cos(3\omega_0 t) + a_4\cos(4\omega_0 t) \qquad \text{per } 0 \le t \le T \\ w(t) \;&=\; 0 \qquad\qquad \text{per } t \text{ qualsiasi} \end{aligned} \tag{1.74}$$

Thus obtaining (see Fig. 1.6):

- rectangular window: $a_0 = 1$; $a_1 = a_2 = a_3 = a_4 = 0$;
- Hanning window: $a_0 = a_1 = 1$; $a_2 = a_3 = a_4 = 0$;
- Kaiser-Bessel window: $a_0 = 1$; $a_1 = 1.298$; $a_2 = 0.244$; $a_3 = .003$;$a_4 = 0$;
- Flat top window: $a_0 = 1$; $a_1 = 1.933$; $a_2 = 1.286$; $a_3 = .388$; $a_4 = 0.32$;

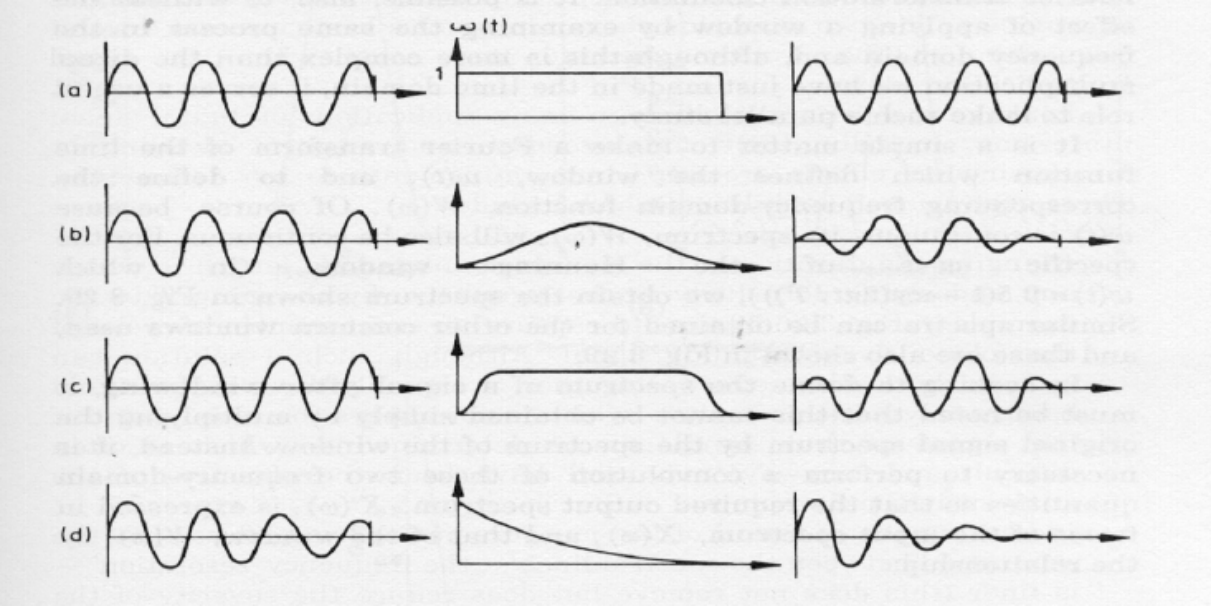

Figure 1.5: Effect of different windows on a harmonic signal in the time and frequency domain

where ω_0 is the fundamental pulsation and the coefficients a_k are chosen so that the areas determined by the different windows are equal.
It is obvious that the rectangular window " weighs " all the data equally, while the other windows, besides returning the initial and final values to zero, also give greater importance to the points that are in the center of the observation window or to the initial values in the case of the exponential window.
With regard to the use of different windows depending on the signal, we have:

- periodic signals: the Hanning window is particularly suitable, while the Kaiser-Bessel window is suitable for frequency selectivity and the Flat-top one for good amplitude determination.
- impulsive signals: the rectangular window is particularly suitable, together with the exponential one; in some cases the Hanning window can be used;
- random signals: the Hanning window is mainly used and in some cases the Kaiser-Bessel window.

1.5.3 Zoom

As we have seen, there is a problem linked to the frequency resolution. In the analyser you can work with a certain number of frequency lines, typically 400, 800, 1600, 3200, 6400, 12800 depending on the number of data you can acquire in the measurement and the frequency resolution is related to the maximum frequency value::

$$\Delta f \;=\; f_{max}/N_R = \frac{f_s}{2N_R} = \frac{1}{2T_sN_R} = \frac{N}{2TN_R} = \frac{2.56}{2T} = 1.28/T \tag{1.75}$$

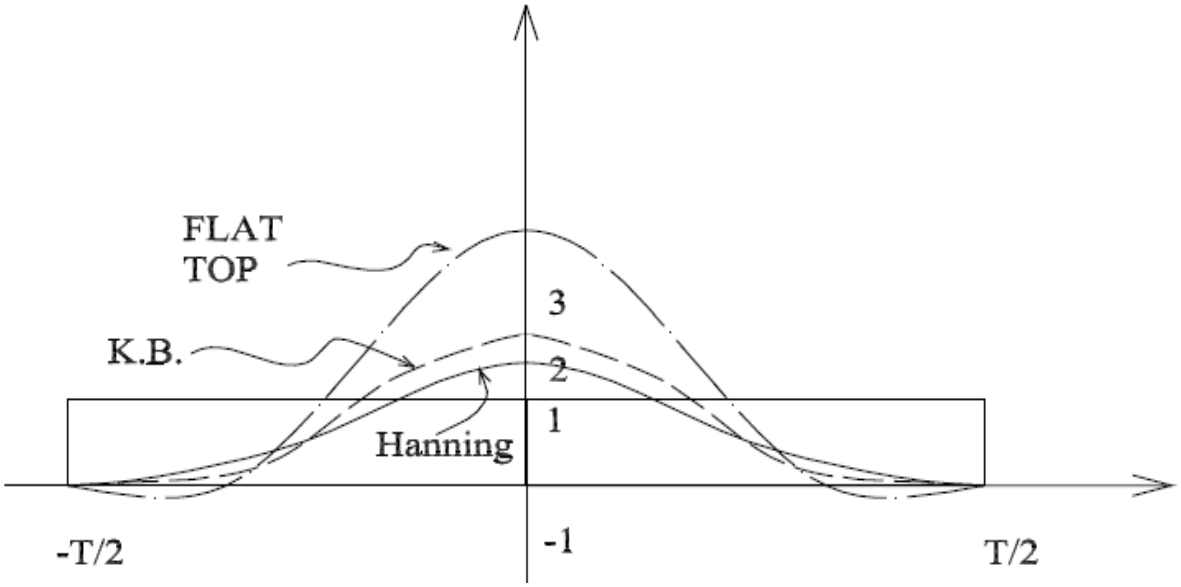

Figure 1.6: Rectangular windows, Hanning, Kaisler-Bessel and flat-top.

where N_R indicates the number of frequency lines and T the observation time; therefore once N_R is fixed, the frequency resolution Δf decreases as the maximum frequency considered for the signal icreases, i.e. ad the frequency bandwidth increases. The number of frequency lines is related to the number of data acquired by the relationship: $N_R = N/2.56$, as already mentioned, a very high resolution in frequency requires a very long observation time.
With the "zoom" it is possible to translate the measurement around the frequency of interest in order. The lines made available by the fast Fourier transform algorithm, which still provides data from zero frequency to the frequency of interest, can be used to obtain a very high resolution. For example, if the signal is simple harmonic:

$$x(t) \;=\; A\sin(\omega t) \tag{1.76}$$

and if it is multiplied by a function:

$$x^*(t) \;=\; \cos(\omega_1 t) \tag{1.77}$$

we get:

$$x_Z(t) \;=\; x(t)\; x^*(t) = \; A\sin(\omega t)\;\cos(\omega_1 t) \tag{1.78}$$

which becomes:

$$x_Z(t) \;=\; \frac{A}{2}\left[\sin[(\omega-\omega_1)t] + \sin[(\omega+\omega_1)t]\right] \tag{1.79}$$

If the higher frequency term is eliminated by filtering, the signal is shifted from its original pulse ω towards a lower pulse ω_1 chosen with the function $x^*(t)$ and thus the signal to be "zoomed", indicated with $x_Z(t)$ is shifted to the pulse $(\omega - \omega_1)$.

There are different techniques for achieving this result, but anyways the time required for signal observation becomes longer in proportion to the zoom factor. It is observed that very small frequency resolution is necessary for structures with very low modal damping coefficients, in order to obtain significant data from several measurement points, and also in the case of closely coupled modes and of structures with fundamental modes at very low frequencies.

1.5.4 Avareging Procedure

The effect of noise on the measurement is reduced by the use of a number, which can also be very high, of successive averages for the evaluation of a single measure; the number of averages is related to the level of statistical reliability we wish to obtain and is limited by the time available and therefore by the "cost" of the measurement. An indication for the evaluation of the number of necessary averages can be found in the measure of the coherence γ^2.
In the case of a random input, an overlapping technique is also used in the evaluation of the averages: the n measures are not obtained with completely different data and therefore with a total observation time equal to nT, if with T is the observation time of a single measure and n the number of averages, but in a time much shorter than nT by using partial superposition in the measurement time. This means that each datum includes a part of the signal already used for the previous measurement, thus reducing the total measurement time: the method is advantageous with respect to the sequential use of the available data, and allows a very high number of averages to be used.

1.5.5 An example of a signal analyzer and generator

The *DIFA DSA (Dynamic Signal Analyzer)* 220 system is a microprocessor based measurement system (see also App. **??**). It can handle up to 20 input channels, each with ICP (Integrated Circuit Piezoelectric), and two output channels for signal generation.
The *D-TAC* (Difa Transfer Analysis and Control software) provides all data acquisition, signal processing and files preparation functions with WIMP-type interface (Windows Icons Menus Pointer).
The software allows the evaluation and presentation of measurement functions in the time and frequency domain with different possibilities.
The *DSA 220* system has 20 input channels, 2 output channels, 1 synchronisation input and an input/output channel: the central processor is an 80486 with 8 MB of RAM and runs under the operating system WINDOWS 3.1.
The DSA system includes three section:

- *data acquisition*: up to 20 input channels, each with signal conditioning, anti-aliasing filtering and analog/digital conversion, A/D.
- *signal processing*: signal filtering and FFT calculation (Fast Fourier Transforms)
- *signal generation*: two output signals from the DSP (Digital Signal Processor), analog and digital filtering techniques, digital/analog conversion, D/A.

Each input channel has an amplifier with adjustable and programmable gain to bring the input voltage up to 32 V_{pp}. ICP type transducers can be connected directly to the input channels.
An *ETD* (Equal Time Delay) filter provides anti-aliasing filtering before sending the signal to

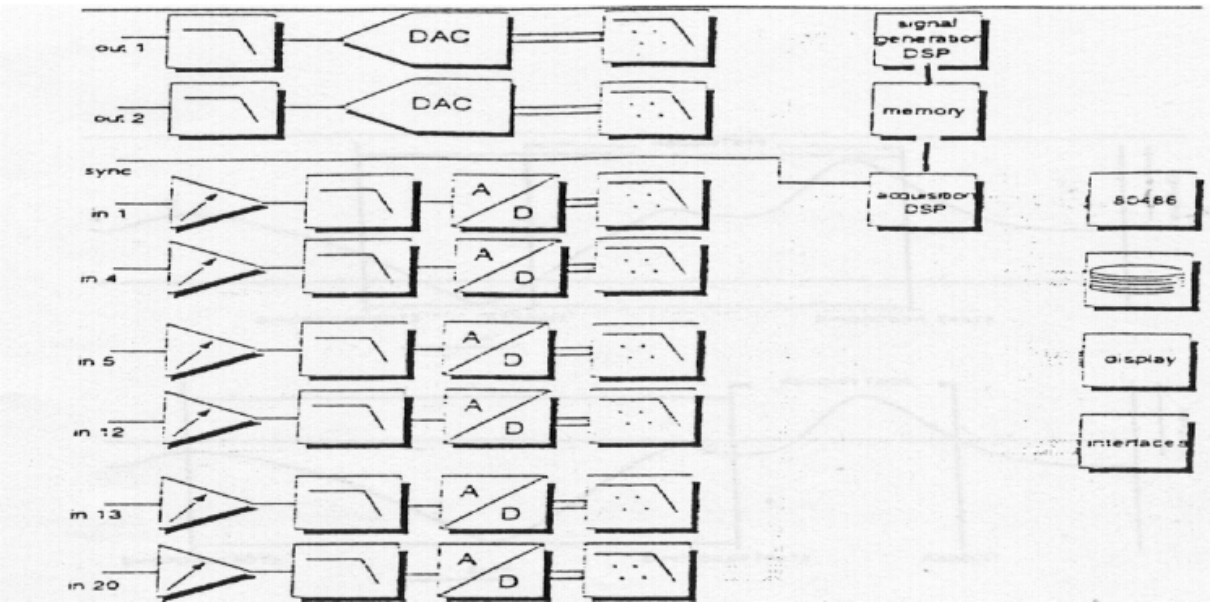

Figure 1.7: Block diagram of the DIFA DSA system.

the *ADC* digital analog converter (Analog Digital Converter), then the signal is sent to the *DSP*. An input for synchronism, *SYNC*,allows an external trigger to be used to initiate data acquisition. The system block diagram is shown in Fig. 1.7. The input channels can bring the output voltage between 100 mV ($200mV_{pp}$) and 16 V ($32V_{pp}$) by means of a gain-adjustable amplifier: the sensitivity can be increased in the measurement of small-level signals and optimal use the analog-to-digital converter, *ADC*, can be done.
An essential point for the correct functioning of the system resides in the anti-aliasing filtering capacity before the analog-digital converter.The anti-aliasing filtering of the *DSA* follows the basic rules:

- no attenuation and linear phase response in the bandwidth, defined at 80% of the Nyquist frequency (which is equal to half the sampling frequency);
- attenuation at -90 dB out of the bandwidth, for complete aliasing elimination.

The anti-aliasing filtering system is automatically adjusted with the choice of the measurement band and therefore with the choice of sampling.
The *DSP* (Digital Signal Processor) section has two dedicated microprocessors: a *Motorola 56001* for data acquisition and an *Analog Devices 2105* for signal generation. To start the measurement, the *DSA* can use different trigger modes; as soon as a measurement is started by the operator, the data are collected by the *DSP* and a routine checks from these data if the triggering condition chosen by the operator is respected: in this case the data acquisition and processing process begins.
Recordings can be chosen in pre- and post-trigger mode, with pre-triggers from 0 to 100% and post-trigger from 0 to 399% of the acquisition block; in Fig. 1.8 examples of pre- and post-trigger conditions are shown.

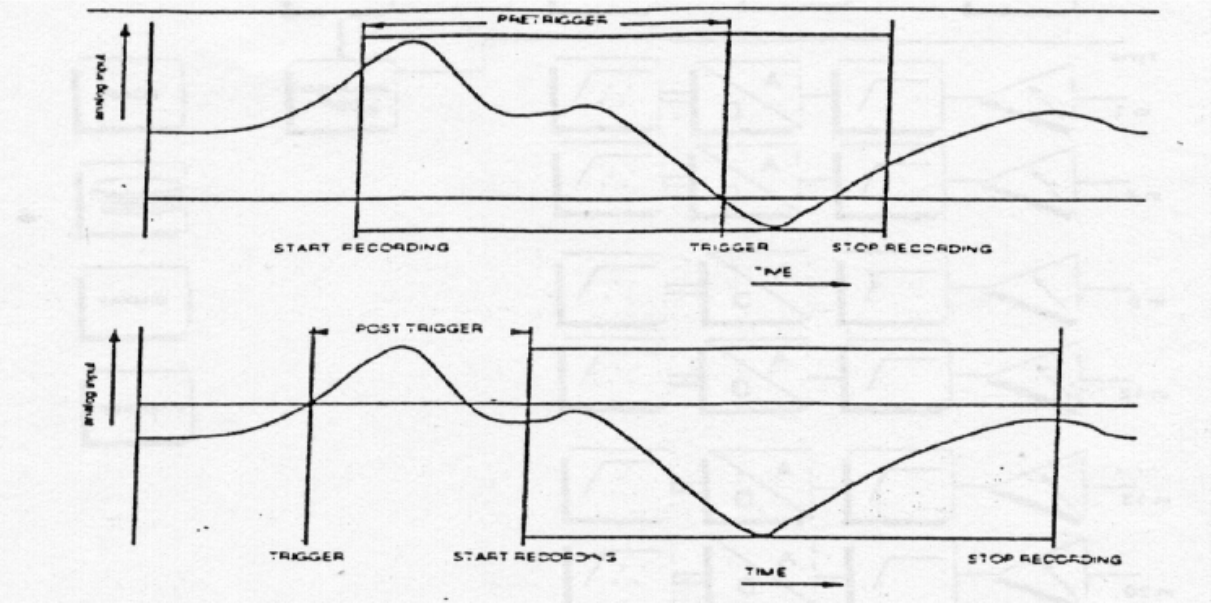

Figure 1.8: Pre and post-trigger conditions.